BL5U

Micro-ARPES Study of the Electronic Structure in Kagome Superconductor $LaRh_3B_2$

T. Kato[1], K. Nakayama[2], T. Osumi[2], S. Souma[1,3], A. Honma[2], K. Tanaka[4,5], T. Takahashi[2] and T. Sato[1,2,3,6,7]

[1]*Advanced Institute for Materials Research (WPI-AIMR), Tohoku University, Sendai 980-8577, Japan*
[2]*Department of Physics, Tohoku University, Sendai 980-8578, Japan*
[3]*Center for Science and Innovation in Spintronics (CSIS), Tohoku University, Sendai 980-8577, Japan*
[4]*UVSOR Synchrotron Facility, Institute for Molecular Science, Okazaki 444-8585, Japan*
[5]*School of Physical Sciences, The Graduate University for Advanced Studies (SOKENDAI), Okazaki 444-8585, Japan*
[6]*International Center for Synchrotron Radiation Innov1ation Smart (SRIS), Tohoku University, Sendai 980-8577, Japan*
[7]*Mathematical Science Center for Co-creative Society (MathCCS), Tohoku University, Sendai 980-8578, Japan*

Ternary rare-earth compounds RT_3X_2 (where R denotes a rare-earth element, T a transition metal, and X typically B, Si, or Ga) are an extensively studied class of intermetallic materials. This family has been attracted attention over the years primarily due to its rich and intriguing physical properties, including various types of magnetic ordering and superconductivity, depending on the specific elemental composition. More recently, stimulated by significant advances in the study of geometrically intriguing kagome lattices, there has been a marked revival of interest in RT_3X_2 compounds, as they feature an ideal kagome lattice formed by the T atoms. The kagome lattice, composed of corner sharing triangles, is known for its potential to host exotic electronic states, such as dispersionless flat bands, linearly dispersing Dirac points analogous to those in graphene, saddle-point van Hove singularity, and topologically non-trivial characters. There is growing interest in elucidating the relationship between the kagome lattice-derived electronic band structures and the physical properties of RT_3X_2 [1]. Nevertheless, despite this renewed focus, the application of experimental techniques capable of directly probing intrinsic electronic states, such as angle-resolved photoemission spectroscopy (ARPES), remains limited for RT_3X_2 [2].

In this work, we have focused on $LaRh_3B_2$, a rare material displaying superconductivity within the RT_3X_2 series. We performed detailed studies of its electronic structure utilizing high-resolution angle-resolved photoemission spectroscopy (ARPES). The experiments were conducted with micro-focused synchrotron radiation beam at beamline BL5U at UVSOR. Clean surfaces necessary for ARPES were obtained by cleaving the crystals *in-situ* in an ultrahigh vacuum better than 1×10^{-10} Torr.

Figure 1 shows representative ARPES data for $LaRh_3B_2$, displaying the second derivative intensity plot measured along the Γ-M high-symmetry line in the hexagonal Brillouin zone (inset) in the normal state (T = 40 K). Our data show multiple hole-like band dispersions centered near the Γ point, whose highest branch approaches the Fermi level (E_F), in agreement with previous work [2]. Our measurements also revealed a hole-like band topped 0.3 eV below E_F at the M point. Through comparing the observed band dispersions with those calculated by density functional theory as well as conducting photon energy dependent ARPES measurements, we found that some of the observed bands are attributed to two-dimensional electronic states at the surface. To clarify the origin of the surface states, we have carried out slab calculations, and found their intriguing electronic and structural properties.

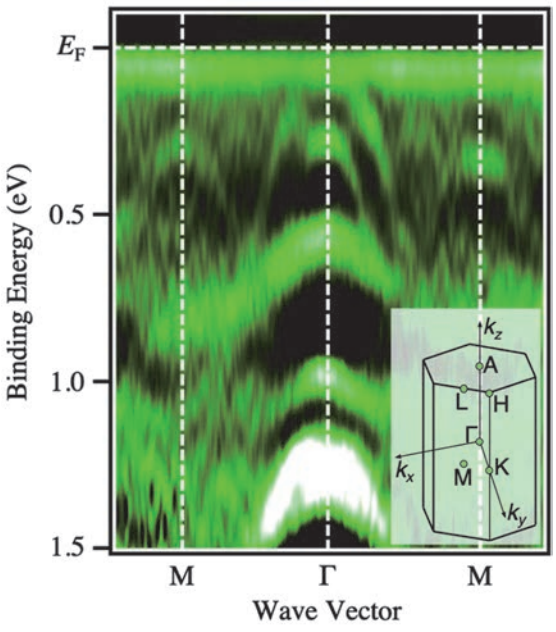

Fig. 1. Plot of second-derivative ARPES intensity measured in the normal state along the ΓM high-symmetry line in $LaRh_3B_2$.

[1] S. Chaudhary *et al*., Phys. Rev. B **107** (2023) 085103.
[2] Y. Iida *et al*., Physica B **351** (2004) 271.

BL5U

Band Structure of Monolayer Germanene Grown on Ag Revealed by ARPES

T. Terasawa[1,2], S.Suzuki[1], D. Katsube[3], S. Tanaka[4] and K. Tanaka[5]
[1]*Advanced Science Research Center, Japan Atomic Energy Agency, Tokai 319-1195, Japan*
[2]*Institute of Industrial Science, The University of Tokyo, Meguro 153-8505, Japan*
[3]*Japan Fine Ceramics Center, Nagoya 456-8587, Japan*
[4]*SANKEN, The Institute of Scientific and Industrial Research, The University of Osaka, Ibaraki 567-0047, Japan*
[5]*UVSOR Synchrotron Facility, Institute for Molecular Science, Okazaki 444-8585, Japan*

Germanene is a monolayer material composed of Ge atoms arranged in a honeycomb lattice. Owing to the spin–orbit interaction in Ge, germanene adopts a buckled atomic configuration. As a result, it is predicted to exhibit a Dirac cone like that of graphene with a high Fermi velocity while also possessing a band gap of 23.9 meV [1]. These characteristics have spurred interest in germanene as a next-generation semiconductor material.

We have developed a novel synthesis method to produce high-quality germanene, as reported by J. Yuhara *et al.* [2]. When an Ag thin film is deposited on a Ge(111) substrate and subsequently heated, Ge atoms diffuse from the substrate to the Ag film surface. Upon cooling, a monolayer germanene forms on the Ag film surface. This segregated germanene exhibits larger domain sizes and long periodic structures. Moreover, the formation of germanene was confirmed by the characteristic Raman peaks unique to germanene [3]. The availability of high-quality germanene can facilitate angle-resolved photoemission spectroscopy (ARPES) measurements. Our ARPES measurements conducted at UVSOR BL5U in 2023 successfully observed germanene-derived bands that are distinct from those of bulk Ag or Ag–Ge alloys [4]. In this work, we aim to further refine these observations by elucidating the band structure of germanene, specifically determining whether the observed bands exhibit a cone-like or saddle-like nature. This distinction is crucial, as in the case of silicene, the saddle-like structure induced by the Ag substrate was often misinterpreted as the π-bands of silicene [5].

Figure 1(a) shows the ARPES intensity map along the Γ-K_{Ge}-M_{Ag} line (kx direction) of germanene grown on an Ag(111) thin film, obtained using 40 eV light. Here, K_{Ge} and M_{Ag} correspond to the K and M points in the Brillouin zone of germanene and Ag(111)-(1×1) surface, respectively. In addition to the prominent Ag 5sp band, a Λ-shaped structure is observed, as indicated by the red broken lines. Figure 1(b) shows the ARPES intensity map for energy (E)-ky plane at kx = 0.9 $Å^{-1}$, corresponding to a white broken line in Fig. 1(a), where the ky direction is perpendicular to the kx direction. The band around -1.5 eV, which corresponds to the Λ-shaped band in Fig. 1(a), exhibits an almost flat but slightly concave-down feature, suggesting that it is not a saddle point but rather a cone-like structure. Therefore, we attributed this band not to the Ag bands but to the π-band of germanene. The difference in the band gradients along kx and ky directions is likely due to the hybridization with Ag.

In summary, we synthesized germanene on the Ag(111) surface by Ge segregation and investigated its electronic structure using ARPES. Our results provide the first indication of a π-band in germanene segregated on Ag(111), as revealed by ARPES intensity maps in both the E-kx and E-ky planes.

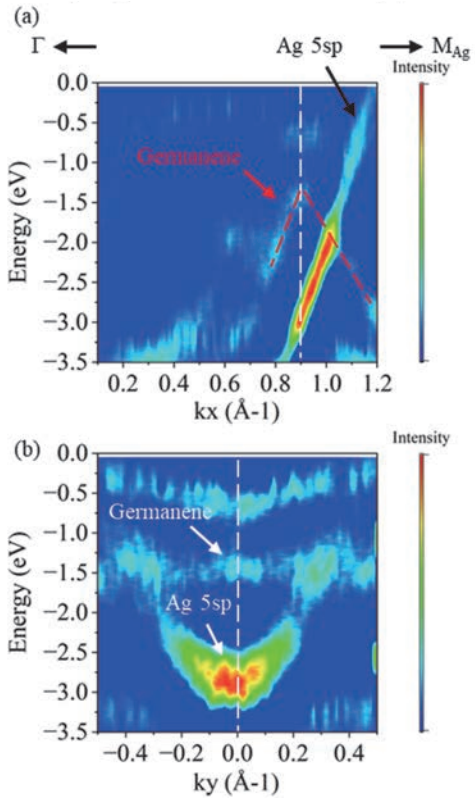

Fig. 1. (a, b) ARPES intensity plots along kx and ky lines. The plots are the second derivative of the raw data to highlight the band features.

[1] C. C. Liu *et al.*, Phys. Rev. B **84** (2011) 195430.
[2] J. Yuhara *et al.*, ACS Nano **12** (2018) 11632.
[3] S. Suzuki *et al.*, Adv. Funct. Mater. **31** (2021) 2007038.
[4] T. Terasawa *et al.*, UVSOR Activity Report **51** (2023) 97.
[5] S. K. Mahatha *et al.*, Phys. Rev. B **89** (2014) 201416.

BL5U

Spin-Polarized Band Mapping in Bi_2Sb_3 Surface States

J. Okabayashi[1] and K. Tanaka[2]

[1]*Research Center for Spectrochemistry, The University of Tokyo, Bunkyo-ku, Tokyo 113-0033, Japan*

[2]*UVSOR Synchrotron Facility, Institute for Molecular Science, Okazaki 444-8585, Japan*

Spintronics is a rapidly emerging field of science and technology that will most likely have a significant impact on the future of all aspects of electronics. Understanding magnetism of surfaces, interfaces, and nanostructures is greatly important for realizing the spintronics which aims to control and use the function of spin as well as the charge of electrons. Spin- and angle-resolved photoemission spectroscopy (spin-resolved ARPES) is one of the most powerful experimental techniques to investigate the magnetic properties of such materials, where one can know the "complete" information of the electronic states of materials, that is, energy, momentum, and spin direction. Recent development of high energy and angle-resolved photoelectron analyzer as well as the contemporary light sources makes it possible for the photoemission spectroscopy to investigate not only band structures but also many body interactions of electrons in solids. However, appending the spin resolution to photoemission spectroscopy is quite difficult because of an extremely low efficiency (10^{-4}) of Mott-type spin detections.

Recently, very low-energy electron diffraction (VLEED-type) spin detector with 100 times higher efficiency than that of conventional Mott-type has been developed and spin-resolved ARPES has been started to be realized [1-3]. So far, most of the spin-resolved ARPES systems are using the single-channel detector and efficiency is still a problem. We have developed high-efficient spin-resolved ARPES system with multi-channel detection (we call "image-spin" detection) to achieve the 100 times better efficiency and the 10 times better momentum resolution than the current spin-resolved ARPES system, which can be a breakthrough in this research field.

Figure 1 displays the ARPES and spin-resolved ARPES images of the topological surface states in Bi_2Sb_3 after cleaving the sample *in-situ* to obtain clean surface. Linearly crossing surface bands at the Dirac points are observed in ARPES, and spin-resolved states for both up and down spin states are distinctly identified with high resolution.

According to rough estimates, the efficiency of spin-resolved ARPES is 100 times greater than that of the single-channel detection systems currently in use worldwide. The imaging detection of spin-resolved mapping can be accomplished using spin manipulation techniques to separate the photoelectrons into up and down spins before their injection into the VLEED target. A new "spin manipulator" can alter the spin direction of the passing electrons in any orientation using adjustable electric and magnetic fields. The installation of the spin manipulator and the optimization of the spin target deposition conditions have significantly enhanced the spin-resolved images, allowing us to achieve spin-resolved images with momentum resolution comparable to that of conventional ARPES.

We are currently fine-tuning the lens parameters of the spin manipulator to capture spin information in the remaining three axial directions. This technique expands the research field by enabling efficient detection of spin-resolved band structures using spin-resolved ARPES.

[1] C. Bigi *et al*., J. Synchrotron Rad. **24**, (2017) 750.
[2] T. Okuda, J. Phys.: Condens. Matter **29** (2017) 483001.
[3] F. Ji *et al.,* Phys. Rev. Lett. **116** (2016) 177601.

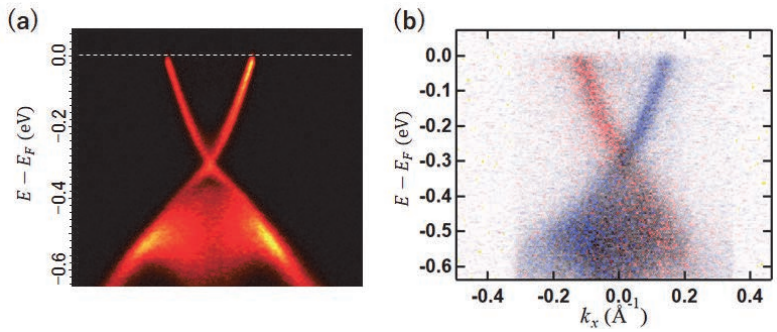

Fig. 1. Band dispersion mapping of Bi_2Se_3 taken at 55 eV photon energy. (a) ARPES and (b) Spin-resolved ARPES.

BL5U

Essential Ingredients for Pseudogap of Electron-Doped Cuprates Studied by Angle-Resolved Photoemission Spectroscopy

M. Miyamoto[1], M. Horio[1], K. Morioya[2], A. Takahashi[3], K. Tanaka[4], Y. Koike[3], T. Adachi[2] and I. Matsuda[1]

[1]*Institute for Solid State Physics, the University of Tokyo, Kashiwa, Chiba 277-8581, Japan*
[2]*Department of Engineering and Applied Sciences, Sophia University, Tokyo 102-8554, Japan*
[3]*Department of Applied Physics, Tohoku University, Sendai 980-85879, Japan*
[4]*UVSOR Synchrotron Facility, Institute for Molecular Science, Okazaki 444-8585, Japan*

It has been widely accepted that, in addition to carrier doping, post-growth reduction annealing process is necessary to induce superconductivity in electron-doped cuprates $R_{2-x}Ce_xCuO_4$ (R: rare earth) with the so-called T'-type structure [1,2]. Neutron-scattering studies suggested that annealing removes excess impurity oxygen atoms at the apical site [3-5]. Stronger annealing, which implies further removal of apical oxygens, enhances the transition temperature T_c [6]. Horio *et al*. found that efficient annealing strongly suppresses the pseudogap, which is believed to compete with superconductivity [7]. The superconducting properties of the T'-type cuprates thus strongly depend on the degree of annealing.

On the other hand, recent studies have stressed the importance of electron doping caused by annealing. Angle-resolved photoemission spectroscopy (ARPES) studies revealed the increase of electron concentration by reduction annealing due to the creation of oxygen deficiencies in the regular sites [7-9]. Song *et al*. [10] reported that the pseudogap depends only on the electron doping level after sufficient reduction annealing. Therefore, the key factor of the pseudogap and superconductivity in electron-doped cuprates remains elusive.

To separate the effects of annealing and electron doping on the electronic structure, we previously carried out ARPES measurements on the as-grown samples of the electron-doped cuprate $Pr_{1.22}La_{0.7}Ce_{0.08}CuO_4$ and doped electrons by K adsorption on the sample surface, which should not influence the crystal structure. As a result, we found the signature of pseuedogap suppression by K adsorption [11]. In this proposal, we performed more detailed investigation into the influence of K adsorption, and also measured $Pr_{1.20}La_{0.7}Ce_{0.10}CuO_4$ annealed sample for comparison, which was annealed with an improved method called dynamic annealing [9,12,13].

ARPES measurements were performed for the as-grown $Pr_{1.22}La_{0.7}Ce_{0.08}CuO_4$ and the annealed $Pr_{1.20}La_{0.7}Ce_{0.10}CuO_4$ samples at BL5U at T = 20 K. By dosing K for the as-grown $Pr_{1.22}La_{0.7}Ce_{0.08}CuO_4$, the Fermi surface transformed from disconnected square shape [Fig. 1(a)] to continuous circular shape [Fig. 1(b)], which indicates pseudogap closing. The energy distribution curves (EDCs) at the node [Fig. 1(c)] and at the hot spot [Fig. 1(d)] show pseudogap suppression after K dosing. The increase in the electron concentration by K dosing estimated from Fermi surface area was approximately 0.12 per Cu site, which shows good reproducibility with previous measurements [11]. We further compared the results with that of the annealed $Pr_{1.20}La_{0.7}Ce_{0.10}CuO_4$ sample and evaluated the influence of apical oxygen removal by reduction annealing.

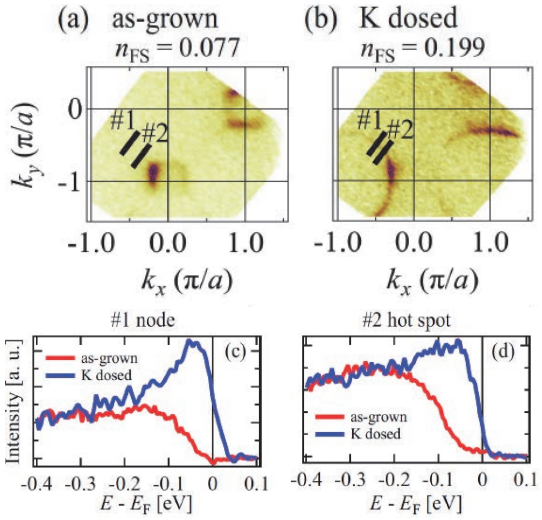

Fig. 1. Fermi surface maps for the as-grown $Pr_{1.22}La_{0.7}Ce_{0.08}CuO_4$ sample (a) before and (b) after K dosing. EDCs at the (c) node and (d) hot spot for each surface condition.

[1] Y. Tokura *et al*., Nature **337** (1989) 345.
[2] H. Takagi *et al*., Phys. Rev. Lett. **62** (1989) 1197.
[3] P. Radaelli *et al*., Phys. Rev. B **49** (1994) 15322.
[4] A. Schultz *et al*., Phys. Rev. B **53** (1996) 5157.
[5] M. Fujita *et al*. J. Phys. Soc. Jpn. **90** (2021) 105002.
[6] J. Kim *et al*., Physica C **209** (1993) 381.
[7] M. Horio *et al*., Nat, Commun. **7** (2016) 10567.
[8] M. Horio *et al*., Phys. Rev. B **98** (2018) 020505.
[9] C. Lin *et al*., Phys. Rev. Research **3** (2021) 013180.
[10] D. Song *et al*., Phys. Rev. Lett. **118** (2017) 137001.
[11] M. Miyamoto *et al*., UVSOR Activity Report **51** (2023) 98.
[12] Y.-L. Wang *et al*., Phys. Rev. B **100** (2009) 094513.
[13] Y. Lee *et al*., J. Phys. Soc. Jpn. **93** (2024) 054701.

BL5U

Resonant ARPES Study for Thermoelectric Property of Layered Ce-Based Compounds

D. Goto[1], K. Kuga[1], M. Matsunami[1,2,3] and T. Takeuchi[1,2,3]
[1]*Toyota Technological Institute, Nagoya 468-8511, Japan*
[2]*Research Center for Smart Energy Technology, Toyota Technological Institute, Nagoya 468-8511, Japan*
[3]*MIRAI, Japan Science and Technology Agency, Tokyo 102-0076, Japan*

The thermoelectric devices, which can convert heat and electricity using Seebeck and Peltier effects, have been considered as one of the most promising choices for energy saving technologies. However, such a thermoelectric generation has not been widely applied due to its low energy conversion efficiency. For evaluating a performance of thermoelectric materials directly related to conversion efficiency, the power factor $PF = S^2/\rho$ where S and ρ are Seebeck coefficient and electrical resistivity, respectively, is frequently used [1]. It is therefore necessary to search for materials possessing large PF by addressing the trade-off relationship between low ρ and large $|S|$.

It is known that in intermetallic compounds called heavy fermion systems, the low ρ and large $|S|$ coexist. This can be caused by the characteristic electronic structure formed by the hybridization between conduction (c) and f electrons. However, in heavy fermion systems, there is a serious problem concerning the sign of S, which cannot be determined solely in terms of the energy dependence of the electron density of states as in most simple metals. Therefore, the energy dependence of the relaxation time and group velocity of quasiparticles, both of which are ignored in many cases [1], should be taken into account.

The main purpose of this research is to establish a methodology for experimentally evaluating the energy dependence of the relaxation time and group velocity of quasiparticles in the vicinity of the Fermi level (E_F) using ARPES. In this study, we focus on the typical heavy fermion systems CeTIn$_5$ (T = Co, Rh, Ir) with a layered crystal structure, which show relatively high large thermoelectric performance at low temperature. In the case of Ce-based compounds, the main part of c-f hybridization bands locates just above E_F in contrast to Yb-based cases. Therefore, for clearly observing the c-f hybridization bands and analyzing them in detail, the photoemission signal Ce 4f electrons should be enhanced by using resonance condition.

Single crystals of CeTIn$_5$ (T = Co, Rh, Ir) were prepared by the In-flux method. Clean sample surfaces were obtained by *in-situ* cleaving. The ARPES measurements were performed at BL5U. The photon energies of 115 eV and 121 eV were selected as the off-resonance and on-resonance condition for Ce 4d-4f edge, respectively. The resonance energy, as generally used in previous studies [2], was also confirmed by our constant initial state (CIS) measurements.

Figure 1 shows the obtained ARPES image of CeCoIn$_5$ (001) surface at 9 K measured with the photon energy of 115 eV (off-) and 121 eV (on-resonance), respectively. The highly dispersive bands due to mainly Co 3d electrons are clearly observed and basically similar between on- and off-resonance condition [2]. The impact of nearly localized Ce 4f electrons is observed at around E_F and 0.25 eV due to spin-orbit splitting, as clearly confirmed in the angle-integrated spectra. From the linewidth of the band dispersion near E_F, the energy dependent analysis for the relaxation time and group velocity of quasiparticles for CeCoIn$_5$ can be determined, and is now in progress.

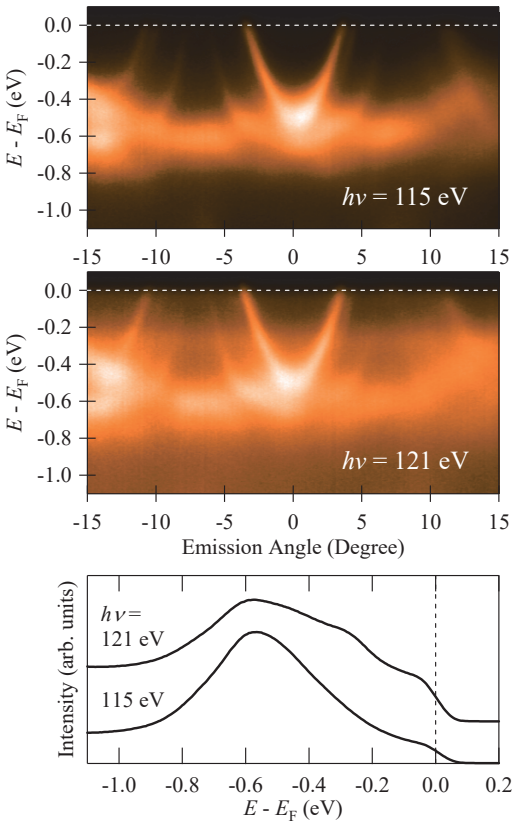

Fig. 1. ARPES image of CeCoIn$_5$ at 9 K measured with photon energies of 115 eV (top) and 121 eV (middle). The bottom figure shows the angle-integrated spectra.

[1] T. Takeuchi, J. Thermoelectrics Soc. Jpn. **9** (2012) 1.
[2] Q.Y. Chen *et al.*, Phys. Rev. B **96** (2017) 045107.

BL5U

Angle-Resolved Photoemission Study of Olivine-Type $LiMnPO_4$ Bulk Single Crystal

T. Ito[1,2], Y. Hatae[1], M. Nakatake[3], S. Takakura[2], K. Tanaka[4,5], Y. Fujiwara[6], T. Taishi[6] and Y. Iriyama[1]

[1]*Graduate School of Engineering, Nagoya University, Nagoya 464-8603, Japan*
[2]*Synchrotron radiation Research center, Nagoya University, Nagoya 464-8603, Japan*
[3]*Aichi Synchrotron Radiation Center, Seto 489-0965, Japan*
[4]*UVSOR Facility, Institute for Molecular Science, Okazaki 444-8585, Japan*
[5]*The Graduate University for Advanced Studies, Okazaki 444-8585, Japan*
[6]*Faculty of Engineering, Shinshu University, Nagano 380-8553, Japan*

With the recent expansion of the use of lithium-ion secondary batteries, development of all-solid-state batteries using lithium-ion conductive inorganic solid electrolytes has been progressing to realize further safety, high energy density, and high output, etc. On the other hand, the valence-band electronic structure, which is essential to understand the relation between lithium-ion and electron conductivity in solid-state energy storage materials, has not been well elucidated yet, though the chemical analysis using operand X-ray photoemission has intensively been applied on the system [1,2]. To clarify the effect of lithium on the electronic structure of cathode material, we have performed angle-resolved photoemission spectroscopy (ARPES) measurements on olivine-type $LiMnPO_4$ [3], which has expected to be potential cathode material with quasi-one-dimensional Li^+ conducting path along the b axis.

ARPES measurements were performed at the UVSOR-III BL5U. Inter-plane ARPES data were acquired at the normal emission angle (θ = 0°) with using hv = 40 - 64 eV at room temperature. To minimize charging effect, we have evaporated K onto the side of sample before cleaving. Single crystals were cleaved in situ along (100) plane.

Figure 1(b) shows photon-energy dependent ARPES spectra of $LiMnPO_4$. For comparison, the density of states (DOS) of $LiMnPO_4$ calculated using density functional theory (DFT) is displayed in Fig. 1(a). From Fig.1(b), we have found that the ARPES peaks show broad dispersive features near the valence band maximum (VBM) around 4 eV and at the band bottom around 10 eV, corresponding to *hv*=62 eV and 50 eV, respectively. It should be noted that K 3p core level around 18.3 eV has not been observed at the cleaved surface, which is suggestive of negligible contribution of evaporated K at the measured spectra.

To show the dispersive features clearly, inter-plane ARPES image along ΓX line of $LiMnPO_4$ is indicated in Fig. 2(a), comparing with DFT calculation (Fig. 2(b)). From the observed symmetry around VBM, the inner potential V_0 is estimated to be 5 eV. Though the complicated dispersive features of Mn 3d-O 2sp hybridized bands have only roughly been observed on the present ARPES results, we expect there are apparent consistency between DFT and ARPES in terms of band gap size (~ 4 eV) and VB width (~ 8 eV). These results suggest the potential utility of ARPES for investigating the electronic structure of cathode material for lithium-ion battery.

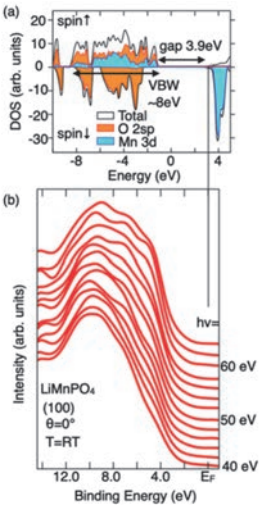

Fig. 1. (a) Density of states of $LiMnPO_4$ [3]. (b) Inter-plane ARPES spectra (θ = 0°) of $LiMnPO_4$.

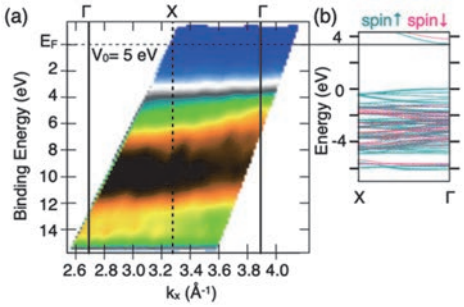

Fig. 2. (a) ARPES image along ΓX line of $LiMnPO_4$. (b) DFT calculations of $LiMnPO_4$ [4].

[1] K. Hikima *et al.*, Commn. Chem. **5** (2022) 52.
[2] K. N. Wood *et al.*, Nature Commun. **9** (2018) 2490.
[3] M. Sgroi *et al.*, Batteries **3** (2017) 11.
[4] The Materials Project. *Materials Data on LiMnPO4 by Materials Project.* United States: N. p., 2020. Web. doi:10.17188/1193777.

BL5U

High-Resolution ARPES of Heavily Overdoped Bi2201 for Evaluation of Coupling Parameters

Y. Miyai[1], S. Ideta[1,2], T. Kurosawa[3], M. Oda[4], M. Arita[2], K. Tanaka[5] and K. Shimada[1,2]

[1]*Graduate School of Advanced Science and Engineering, Hiroshima University, Higashi-Hiroshima 739-0046, Japan.*

[2]*Hiroshima Research Institute for Synchrotron Radiation Science (HiSOR), Hiroshima University, Higashi-Hiroshima 739-0046, Japan*

[3]*Faculty of Science and Engineering, Muroran Institute of Technology, Muroran 050-8585, Japan*

[4]*Department of Physics, Hokkaido University, Sapporo 060-0809, Japan*

[5]*UVSOR Synchrotron Radiation Facility, Institute for Molecular Science, Okazaki 444-8585, Japan*

High transition-temperature (T_c) cuprate superconductors have attracted much interest since their discovery. While there have been extensive studies, there exist unsettled physical phenomena such as bad metal, density waves, magnetic fluctuations, and nematic phases [1-4]. These states are emergent from the competing charge, spin and lattice degrees of freedoms. To understand the origin of the physical properties of cuprates, it is desirable to disentangle these competing interactions and quantify each contribution. To this end, here we focus on the Bi-based high-T_c cuprate, $(Bi,Pb)_2Sr_2CuO_{6+\delta}$ (Bi2201). The Fermi surface of Bi2201 is relatively simple because there exists a single CuO_2 layer in the unit cell. In this study, we start from the overdoped region, where the electronic state is expected to behave as the Fermi Liquid [3]. However, recently, Kurashima *et al*. found a ferromagnetic fluctuation close to the vanishing T_c region, and the ground state properties in this region should be investigated [3]. Previously Meevasana *et al*. have done angle-resolved photoemission spectroscopy (ARPES) and examined the self-energy due to the electron-electron and electron-phonon interactions especially for the heavily overdoped Bi2201 with no superconducting transition [5]. However, each contribution from the electron-phonon (or electron-boson) and electron-electron interactions as a function of hole concentration is still not clearly determined. Our purpose is, therefore, to systematically clarify the evolution of these interactions as a function of hole concentrations.

To quantitatively evaluate the electron-boson interaction and the electron-electron interaction, we have focused on the Bi-based high-T_c cuprate, Pb-Bi2201 and performed high-resolution ARPES at BL5U. The low T_c (~6 K) allows us to evaluate the normal self-energy at low temperature by suppressing the thermal broadening. In addition, the Pb doping suppresses the structural modulations of the BiO layer and hence the superstructure reflections in the ARPES spectra, and therefore, the overdoped sample is expected to behave like metals enable us to extract normal self-energy. We clearly observed a parabolic quasiparticle dispersion in the nodal direction [7]. By applying tight-binding (TB) model, and we found that the evaluated real part of the self-energy crosses the zero point around $\omega \sim -0.6$ eV, where the imaginary part of the self-energy takes the minimum. The self-energy part responsible for the high-energy anomaly (HEA) is almost temperature independent and the coupling parameter is $\lambda_{HEA} \sim 1$ at 300 K, indicating strongly correlated nature of the strange metal state. We have also measured fine details near the Fermi level using the μ-Laser ARPES machine and have observed a clear kink structure around -90 meV. From this experiment, we found that, the self-energy part responsible for the low-energy kink (LEK) near the Fermi level shows significant temperature dependence: it is $\lambda_{LEK} \sim 0.1$ at 300 K but enhances steeply below ~150 K up to $\lambda_{LEK} \sim 0.8$, leading to the total coupling strength of $\lambda_{tot} = \lambda_{HEA} + \lambda_{LEK} = 1.8$ at 20 K.

In this study, we evaluated the self-energy due to the electron-phonon and electron-electron interactions using the two band TB model. Comparing the theoretical results, the high-energy anomaly is considered to originate from local excitations that are characterized by spin fluctuation or charge fluctuation. Our results clearly indicate distinct energy scales in the self-energy, providing insight into the strange metal state as well as the temperature-dependent interactions of many-body interactions. The details of this study have been published in Ref. [6].

[1] P. Choubey *et al*., PNAS, **117** (2020) 14805.
[2] Y.Y. Peng *et al*., Nature Materials **17** (2018) 697.
[3] K. Kurashima *et al*., Physical Review Letters **121** (2018) 057002.
[4] N. Auvray *et al*., Nature Communications **10** (2019) 5209.
[5] W. Meevasana *et al*., Physical Review B **75** (2007) 0174506.
[6] Y. Miyai *et al*., Phys. Rev. Research **7** (2025) L012039.

BL5U

Electronic Structure Modulation in the CDW Phase of Kagome Superconductor AV_3Sb_5 Studied by ARPES

K. Nakayama[1], S. Suzuki[1], T. Kato[2], Y. Li[3,4,5], Z. Wang[3,4,5], S. Souma[2,6], K. Tanaka[7,8], T. Takahashi[1], Y. Yao[3,4] and T. Sato[1,2,6,9,10]

[1]*Department of Physics, Graduate School of Science, Tohoku University, Sendai 980-8578, Japan*
[2]*Advanced Institute for Materials Research (WPI-AIMR), Tohoku University, Sendai 980-8577, Japan*
[3]*Centre for Quantum Physics, Key Laboratory of Advanced Optoelectronic Quantum Architecture and Measurement (MOE), School of Physics, Beijing Institute of Technology, Beijing 100081, P. R. China*
[4]*Beijing Key Lab of Nanophotonics and Ultrafine Optoelectronic Systems, Beijing Institute of Technology, Beijing 100081, P. R. China*
[5]*Material Science Center, Yangtze Delta Region Academy of Beijing Institute of Technology, Jiaxing 314011, P. R. China*
[6]*Center for Science and Innovation in Spintronics (CSIS), Tohoku University, Sendai 980-8577, Japan*
[7]*UVSOR Synchrotron Facility, Institute for Molecular Science, Okazaki 444-8585, Japan*
[8]*School of Physical Sciences, The Graduate University for Advanced Studies (SOKENDAI), Okazaki 444-8585, Japan*
[9]*International Center for Synchrotron Radiation Innovation Smart (SRIS), Tohoku University, Sendai 980-8577, Japan*
[10]*Mathematical Science Center for Co-creative Society (MathCCS), Tohoku University, Sendai 980-8578, Japan*

The kagome lattice provides a rich platform for the exploration of unconventional quantum phenomena, including Weyl semimetals, chiral density-wave orders, fractional charges, and exotic superconductivity. These arise from the interplay of electron correlation effects with unique electronic band features like flat bands, Dirac cones, and van Hove singularities. The recently discovered materials AV_3Sb_5 (A: an alkali metal), characterized by vanadium atoms forming an ideal two-dimensional kagome network, offer a valuable opportunity to explore novel physics within the kagome lattice structure [1].

AV_3Sb_5 exhibits the charge-density wave (CDW) state defined by three-dimensional lattice distortions with a periodicity of 2 × 2 × 2 or 2 × 2 × 4, depending on the A element. The CDW transition temperature, T_{CDW}, varies according to the alkali metal, ranging from 78 K to 103 K. Within this CDW phase, AV_3Sb_5 materials often display a breaking of not only translational symmetry but also rotational symmetry. The latter phenomenon suggests the emergence of nematic states, which have occasionally been identified in strongly correlated electron systems, such as cuprates and iron-based superconductors. To verify this nematicity and elucidate its origin, a detailed investigation of the electronic band structure is essential.

In this study, we have performed high-resolution angle-resolved photoemission spectroscopy (ARPES) measurements of a series of AV_3Sb_5 (A = K, Rb, and Cs). High-resolution ARPES measurements were performed at BL5U with linearly polarized photons of 90-150 eV.

Figure 1 shows a representative band dispersion measured in the CDW state of KV_3Sb_5. Compared to the normal state, we observed doubling of some energy bands, which indicates CDW-induced electronic reconstruction [2,3]. We performed first-principles band calculations to understand the observed band doubling and found it originates from the formation of staggrred three-dimensional CDW order. This CDW state naturally breaks rotational symmetry, resulting in nematic-like responses. To amplify the nematic-like response, we developed uniaxial strain device compatible with ARPES, and studied impact of uniaxial strain on the electronic structure.

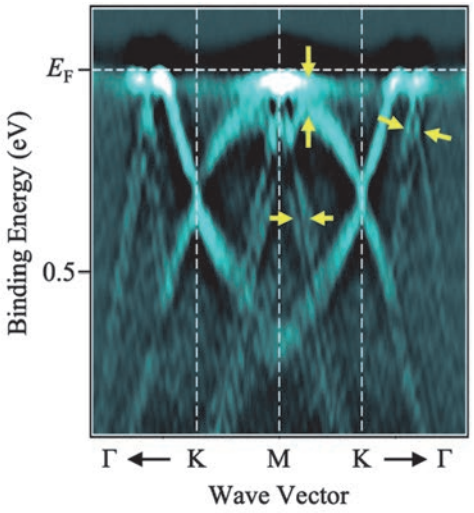

Fig. 1. Second-derivative ARPES intensity plot measured in the CDW state in KV_3Sb_5.

[1] Y. Zhong, J.-X. Yin and K. Nakayama, J. Phys. Soc. Jpn. **93** (2024) 111001.
[2] K. Nakayama *et al.*, Phys. Rev. B **104** (2021) L161112.
[3] T. Kato *et al.*, Commun. Mater. **3** (2022) 30.

BL5U

Explorations of Bandgap-Tuned Excitonic Insulator Materials by Angle-Resolved Photoemission Spectroscopy

K. Fukutani[1,2], R. Nakazawa[1], S. Makita[1], K. Tanaka[1,2] and S. Kera[1,2,3]

[1]*Institute for Molecular Science, Okazaki 444-8585, Japan*

[2]*School of Physical Sciences, The Graduate University for Advanced Studies, Okazaki 444-8585, Japan*

[3]*Graduate School of Science and Engineering, Chiba University, Chiba 263-8522, Japan*

An exciton, a bound pair of an electron and a hole, is one of the most fundamental quasiparticles in condensed matters, which forms as a result of external excitations, such as light irradiations, and plays a pivotal role not only in various electronic devices, including photovoltaic cells and light-emitting diodes, but also in biological processes like photosynthesis.

On the other hand, it is interesting to point out that in the most naïve picture, the negatively charged electrons and positively charged holes would naturally attract each other, and one may expect their bound state (excitons) to be stable in the ground state of matters. Of course, this view is, generally speaking, incorrect in that excitons would *not* form spontaneously in most materials. This is, roughly speaking, due to the effect of electrostatic screening arising from the sea of charged particles, which needs to be properly accounted for when the many-body ground state is to be determined. As it turns out, for most materials, the effect of screening is strong enough to make the binding of electrons and holes energetically more expensive than when they remain separated.

Extending along the line of thought mentioned above, an interesting question can be proposed; that is, what if we tune the bandgap of materials so as to decrease the density of carriers (i.e., source of screening) across the limit where the simple electron- hole Coulomb attraction can overcome the "barriers" of carrier screening? This question is pondered by N. F. Mott, W. Kohn, D. Jerome and others, and have led to the theoretical prediction of what is called an *excitonic insulator* (EI) [1], in which the simple Coulomb attraction between the electrons and holes manifests itself as they form a condensate of excitons in the many-body ground state.

While the charge neutrality of excitons and the lack of distinct macroscopic behaviors like superfluidity had made it difficult for the experimental probes to unambiguously detect the EI phase, various prominent candidate materials exist, such as Ta_2NiSe_5 and $TiSe_2$. In particular, $TiSe_2$ has been proposed as an EI material nearly two decades ago [2] and have been extensively investigated by various experimental probes. Nonetheless, due to the presence of both the exciton and the phonon degrees of freedom, which are closely interlinked near the quantum criticality, its true nature is still under disputes and a general consensus has not been reached.

Thus, we once again trace back to the original question of how the bulk carrier density (closely linked to the magnitude of bandgap) affects the competition between the electron-hole Coulomb attraction and the carrier screening. In our experiments, we have performed the photon-energy- and polarization-dependent angle-resolved photoemission spectroscopy (ARPES) on $Ti(Se_{1-x}Te_x)_2$, to observe the evolution of their 3D band structures. As shown in Fig. 1, the negative bandgap is clearly enhanced as the Te-doping x increases from 0 to 0.5 and at the same time, the charge density wave, believed to be accompanied by the EI transition, is confirmed to be suppressed down to T = 5 K. Further investigations on various Te-doping concentrations are expected to provide important insights into one of the fundamental questions in many-body condensed matter physics.

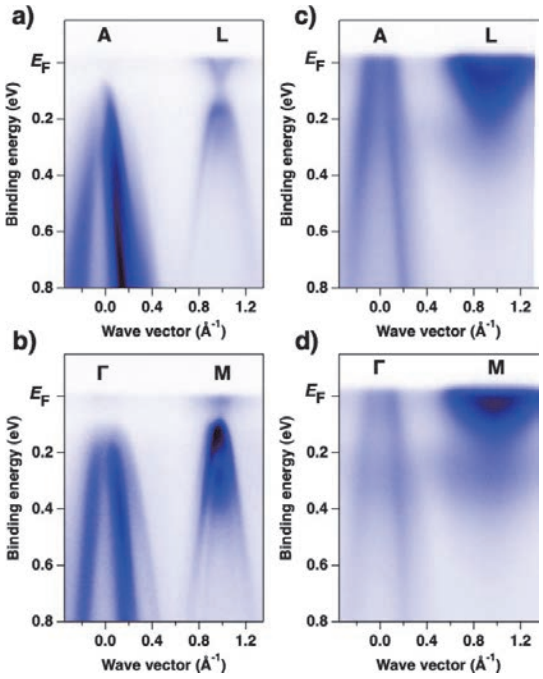

Fig. 1. ARPES intensity plots for $TiSe_2$ (x = 0) taken at (a) $h\nu$ = 44 eV, (b) $h\nu$ = 58 eV and TiSeTe (x = 0.5) taken at (c) $h\nu$ = 44 eV, (d) $h\nu$ = 58 eV near the indicated high-symmetry lines of bulk Brillouin zones at T = 10 K.

[1] D. Jerome *et al*., Phys. Rev. **158** (1967) 462 etc.
[2] H. Cercellier *et al*., Phys. Rev. Lett. **99** (2007) 146403 etc.

BL5U

Relation between Electronic Structure and Thermopower in $YbCu_2Si_2$

D. Goto[1], S. Uchida[1], M. Matsunami[1,2,3] and T. Takeuchi[1,2,3]
[1]*Toyota Technological Institute, Nagoya 468-8511, Japan*
[2]*Research Center for Smart Energy Technology, Toyota Technological Institute, Nagoya 468-8511, Japan*
[3]*MIRAI, Japan Science and Technology Agency, Tokyo 102-0076, Japan*

Thermoelectric technology, which is capable of converting temperature differentials directly into electrical energy, can maximize the efficient use of existing energy sources. However, thermoelectric generation has not been widely applied in our society due to its energy conversion inefficiency. As evaluation criteria for the efficiency, the dimensionless figure of merit $ZT = S^2T/\rho\kappa$ or the power factor $PF = S^2/\rho$ where S, ρ, and κ are the Seebeck coefficient, electrical resistivity, and thermal conductivity, respectively, of constituent materials, are well known. It is necessary to search for materials possessing large ZT or PF.

It is known that in heavy fermion systems, the low ρ and large $|S|$ coexist, resulting in a large PF. This can be caused by the characteristic electronic structure formed by the hybridization between conduction and f electrons. However, there is a serious problem concerning the sign of S, which cannot be determined solely in terms of the energy dependence of the electron density of states as in most simple metals. Therefore, the energy dependence of the relaxation time of quasiparticles, both which are the terms in Mott formula and are neglected in many cases, should be taken into account.

The main purpose of this research is to establish a methodology for experimentally evaluating the energy dependence of the relaxation time of quasiparticles in the vicinity of the Fermi level (E_F) using angle-resolved photoemission spectroscopy (ARPES). In this study, we focus on the typical heavy fermion system $YbCu_2Si_2$, which is known to show relatively high large $|S|$ [1].

Single crystals of $YbCu_2Si_2$ were prepared by the Sn-flux method. The elements, Yb (3N) Cu (4N), Si (5N), and Sn (3N), with an off-stoichiometric ratio of Yb : Cu : Si : Sn = 1 : 15 : 2 : 50 were inserted in an alumina crucible and sealed in a quartz tube. The quartz tube was heated to 1050 °C, maintained at this temperature for two days, and cooled to 600 °C at the rate of 2 °C/h, taking about 12 days in total. The excess flux was removed using a centrifuge outside the furnace. Synchrotron ARPES measurements were carried out at the undulator beamline BL5U of UVSOR facility in the Institute for Molecular Science, using photon energies of 40 eV - 121 eV and a hemispherical electron analyzer, MBS-A1. The total energy resolution was set to 21 meV for a photon energy of 40 eV. The clean (001) surface of single crystals was obtained by *in-situ* cleaving under ultra-high vacuum condition. The Fermi level was determined by measuring a polycrystalline gold film in electrical contact with the samples.

The inset of Fig. 1 shows the Brillouin zone of $YbCu_2Si_2$. In the present study, the ARPES image is measured along the directions from Γ to X or from Z to X in the neighboring Brillouin zone corresponding to the $\bar{\Gamma}$-$\bar{X}$ direction in the surface Brillouin zone. Figure 1 shows the Fermi surface measured with a photon energy of 40 eV. According to the band calculation (LDA + U) [1], $YbCu_2Si_2$ has at least two Fermi surfaces, in which one is due to quasi two-dimensional (33th) electron band centered at X point focused in the present study and the other is due to three-dimensional (32th) hole band around Z point. By analyzing these bands, we will further investigate the relation between the electronic structure and Seebeck coefficient in $YbCu_2Si_2$.

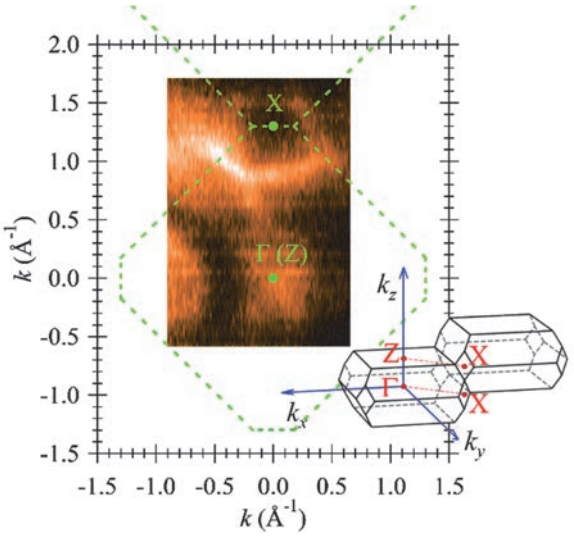

Fig. 1. (a) ARPES image of $YbCu_2Si_2$ along $\bar{\Gamma}$-$\bar{X}$ direction at 9 K measured with the photon energy of 121 eV.

[1] N.D. Dung *et al.*, J. Phys. Soc. Jpn. **78** (2009) 084711.
[2] M. Matsunami *et al.*, Phys. Rev. B **87** (2013) 165141.

Electronic Structure Study on Novel Spin-Split Collinear Antiferromagnets

Z. Lin[1], X. Liang[1] and J. Ma[1]
[1]*Department of Physics, City University of Hong Kong, Kowloon, Hong Kong, China*

Magnetism, a foundational domain in condensed matter physics, conventionally classifies magnetic materials into two primary phases: ferromagnets and antiferromagnets (although unconventional forms like ferrimagnetism and chiralmagnetism are also recognized). Ferromagnets exhibit macroscopic magnetization in spatial space and spin splitting in reciprocal momentum space.

Conversely, typical antiferromagnets show no net macroscopic magnetization in spatial space and no spin splitting in reciprocal momentum space when time reversal symmetry combined with inversion or translation operation is preserved [1–3]. Recent theoretical investigations have identified special collinear antiferromagnetic materials with substantial spin-split band structures but no net macroscopic magnetization. This has led to the proposal of altermagnetism, a special antiferromagnetic phase that appropriately describes such materials. In contrast to conventional antiferromagnets, which have spin sublattices linked to one another through straightforward translation operations, altermagnetism involves linking sublattices with opposite spins using rotation operations. Applying the same rotational angle in momentum space causes a spin flip between up and down. As outcome of this phenomenon, even-order wave symmetries of the spin pattern appear, such as the d-, g-, and i-waves. Recently, it has even been suggested that altermagnetism can extend to include non-collinear spins and multiple local-structure variations.

In this study, we focus on d-wave altermagnet candidate RuO_2 and g-wave altermagnet candidate CrSb. We have carried out high-resolution spin angle-resolved photoemission spectroscopy (ARPES) measurements of RuO_2 and CrSb by using MBS-A1 spectrometer and customized VLEED spin detector at BL5U.

Figure 1 and 2 shows the spin ARPES result of this beamtime. Figure 1 shows that RuO_2's spin texture is symmetric about the Γ point, which conflicts with the presented result [4]. The result in Fig.1 indicates that the spin texture of RuO_2 is not from space-inversion symmetry breaking. Figure 2 shows the possible spin splitting band structure of CrSb.

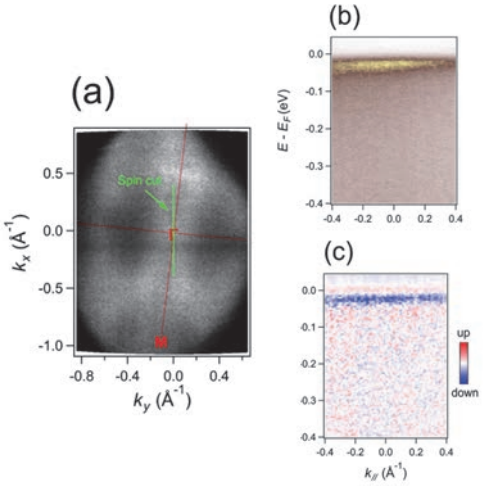

Fig. 1. (a), Fermi Surface of RuO_2. (b), The ARPES band structure of the green line in Fig. 1(a). (c), The spin resolved data of the same path band structure as (b).

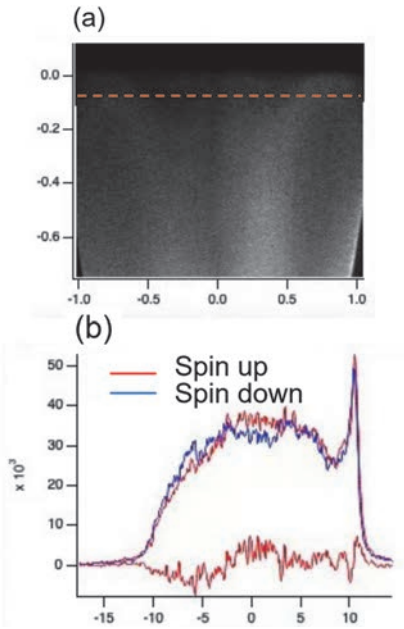

Fig. 2. (a), a high-symmetric path's band structure of CrSb. (b), The spin resolved MDC of the orange line of figure 2(a).

[1] L. Néel, Science **174** (1971) 985.
[2] L. Šmejkal, J. Sinova, and T. Jungwirth, Phys. Rev. X **12** (2022) 031042.
[3] L. Šmejkal, J. Sinova, and T. Jungwirth, Phys. Rev. X **12** (2022) 040501.
[4] J. Liu *et al*., Phys. Rev. Lett. **133** (2024) 176401.

BL5U

Photoemission Study about the Fermi Arc in Type-II Weyl Semimetal $NbIrTe_4$

S. Cho[1] and D. Shen[2]
[1]*Department of Physics Education, Sunchon National University, Suncheon57922, Republic of Korea*
[2]*National Synchrotron Radiation Laboratory, University of Science and Technology of China, Hefei 230026, China*

The unique features of topological Weyl semimetals (TWSs) arise primarily from their unusual band structure around the Weyl nodes and the topologically non-trivial surface state as Fermi arc, which connect each pair of Weyl nodes [1]. Moreover, TWSs have a family so-called type-II TWSs, where the Weyl nodes are highly anisotropic and tilted, breaking the Lorentz symmetry [2]. The Weyl nodes of type-II TWSs appear as contact points between electron and hole pocket in the bulk band structure, which result in the presence of the boundaries between these pockets. One of the promising candidates for type-II TWSs is WTe_2, which has the orthorhombic crystal structure with space group $Pmn2_1$ and the bulk system of WTe_2 exhibits the non-saturating magnetoresistance [2].

Recently, $NbIrTe_4$ and $TaIrTe_4$, which crystallize in the non-centrosymmetric orthorhombic space group $Pmn2_1$ (No. 31), have been suggested as possible type-II TWSs. The previous calculation result of $NbIrTe_4$ revealed a closed Fermi arc loop that connects two distinct pairs of Weyl nodes from the top and bottom surfaces in the type-II TWSs [3]. Given the symmetry of $TaIrTe_4$ (presence of time-reversal symmetry but with broken inversion symmetry) and the Berry curvature originating from its type-II Weyl nodes, $TaIrTe_4$ can expect to exhibit a large and room-temperature nonlinear Hall effect [4]. Moreover, the recent scanning tunneling microscopy results of $TaIrTe_4$ show a superconducting gap below a critical temperature 1.54 K [5]. The behavior of the normalized upper critical field and the stability of the superconductivity against the ferromagnetism suggest the unconventional superconductivity with the p-wave pairing. The results of the scanning tunneling spectroscopy and angular-dependent transport measurements show that the superconductivity is the quasi-1D and occurs in the surface states [5].

Here, we investigate the spin structure of the Fermi arc associated with the type-II Weyl nodes in $NbIrTe_4$. Given the lack of inversion symmetry, $NbIrTe_4$ is predicted to host four type-II Weyl nodes. In previous band calculation, one of these type-II Weyl points was found to show an intersection of tilted cone which lies on the Fermi energy at $E - E_F = 0.131$ eV. The electronic structure of $NbIrTe_4$ shows the different surface state at two different surface terminations (top and bottom surface in Fig. 1a), leading to distinct Fermi arc loop configuration. This is because the Fermi arc loop connects different pairs of the Weyl nodes depending on the surface termination.

Figure 1 (b) and (c) show the Fermi surface and the band structure at $k_y = 0$ (red dotted line in Fig. 1b) taken from the bottom surface termination. The Fermi arc exists near the Γ-point, consistent with the previous band calculation results in Ref. [3]. We try to measure the spin structure of the Fermi arc in Fig. 1 (d). Figure 1 (d) shows the spin-resolved momentum distribution curves (MDC) and spin polarization of the Fermi arc at EB = -0.01 eV. We found that the spin polarization taken from the left and right momentum points show opposite direction of s_y with red and blue assigned for spin-down and spin-up respectively. We hope our results on the spin-resolved MDC may provide valuable insights into the characteristics of type-II Weyl nodes.

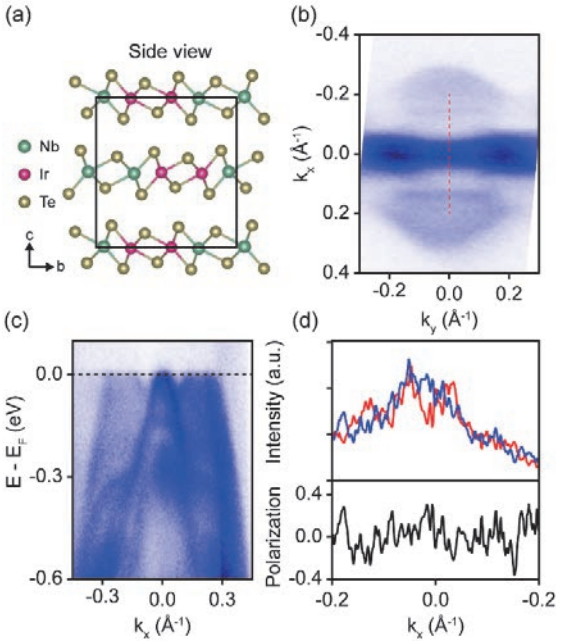

Fig. 1. (a) Crystal structure of $NrIrTe_4$ (b) The Fermi surface obtained from the bottom surface termination. (c) The band structure at the red line in b. (d) spin-resolved MDC along the s_y direction and the spin polarization at $E_B = -0.01$ eV.

[1] A. Bansil, H. Lin, and T. Das, Rev. Mod. Phys. **88** (2016) 021004.
[2] A. A. Soluyanov *et al*., Nature **527** (2015) 495.
[3] S. A. Ekahana *et al*., Phys. Rev. B **102** (2020) 085126.
[4] D. Kumar *et al*., Nat. Nanotechnol. **16** (2021) 421.
[5] Y. Xing *et al*., Natl. Sci. Rev. **7** (2020) 579.

BL5U

Growth of P Ultra-Thin Film on Cu(111)

N. Maejima[1] and T. Yokoyama[1]
[1]*Institute for Molecular Science, Myodaiji-cho, Okazaki 444-8585, Japan*

Two-dimensional single-element materials, such as graphene, silicene and germanene etc., have attracted much attention owing to their unique physical and chemical properties. Phosphorene, has attracted attention due to its high mobility and variable band gap depending on the number of atomic layers. Blue phosphorene with a Dirac cone, produced by evaporation of P on a heated Cu(111) substrate, was recently reported [1]. The 1 ML and 1.5 ML blue phosphorene samples show 10√3x 10√3 and 13 x 13 moire LEED patterns, respectively. The formation of self-assembled P nanodots on top of the phosphorene sheet of 13x13 sample was clearly observed in the study. In this report,1ML phosphorene was grown on Cu(111) which shows 13x13 moire LEED pattern in different fabrication process.

Experiments were performed at BL5U of the UVSOR facility. The Cu(111) surface was cleaned by cycles of Ar^+ ion spattering (0.75 keV) and annealing (600 °C). P atoms were deposited by directly heating of a piece of GaP wafer. The Cu(111) substrate was kept at 300 °C during the P atoms deposition. The prepared Cu(111) and P deposited Cu(111) samples showed 1x1 and 13x13 moire LEED patterns, respectively. The P deposited sample were post-annealed at 500°C. The LEED pattern was not changed from of this sample consisted of 1x1 spots arising from 13x13 moire LEED pattern. P 2p and valence band photoelectron spectroscopy (PES) measurements were performed by an MBS A-1 analyzer.

Figure 1 shows the P 2p spectrum obtained from P deposited during 300°C annealing and 500°C post-annealing samples with black and red solid lines, respectively. In the spectrum of the P deposited sample during 300°C annealing, P 2p 3/2 peak of shoulder and main components were observed at 128.3 eV and 128.8 eV, respectively. These peak components were attributed to the P nanodot and blue phosphorene layer, respectively, in the previous study [1]. The 500°C post-annealing sample have only the main component at 128.8 eV. The total area of the P 2p spectrum was reduced to 80% by 500°C post- annealing process. The P nanodot component observed in the spectra of 300°C annealing sample has disappeared, indicating that the whole surface is simply covered with blue phosphorene monolayer. The band dispersion of the valence band of the sample post-annealed at 500 °C showed a linear band around the Cu(111) $\overline{K}$ point. This result is similar to the band structure of 10√3x10√3 1ML Blue Phosphorene sample structure previously reported. Combining these results and the fact that the LEED pattern was not changed by the 500 °C post-annealing process indicates that the 13x13 structure is not due to nanodot origin but to a blue phosphorene monolayer. There are several lattice constants for phosphorene reported ranging from 3.4 Å to 4.2 Å [1]-[3]. Such flexible lattice constants are attributed to differences in the planarity of the phosphorene layers and surface super structure.

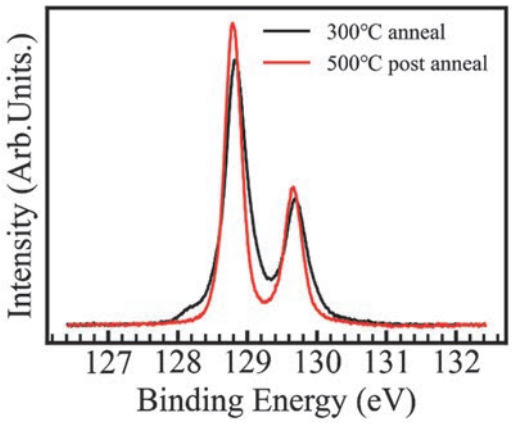

Fig. 1. Figure 1 shows the P 2p spectrum of P deposited during 300°C annealing (black solid line) and 500°C post- annealing samples (red solid line).

[1] Y. Kaddar *et al., Adv. Funct. Mater.* **33** (2023) 2213664.
[2] YH. Song, *et al.,* Nat Commun. **15** (2024) 1157.
[3] D. Zhou, *et al.,* ACS Nano **14** (2020) 2385.

Spin-Resolved Electronic Structure of Altermagnet MnTe and CrSb

M. Zeng[1] and C. Liu[1]
[1]*Southern University of Science and Technology (SUSTech), Shenzhen, Guangdong 518055, China*

Magnetic materials play a crucial role in modern technology, and controlling spins in these materials remain a central challenge in spintronics [1–3]. Large spin-splitting has been observed primarily in ferromagnetic materials and system with strong spin-orbit coupling (SOC). However, strong SOC is typically found in heavy elements, which are often toxic and prone to defects, limiting their practical applications.

Recently, researchers have discovered that light-element collinear antiferromagnets could also exhibit properties that are traditionally inherit to ferromagnets [4–9]. In these systems, SOC is negligible, allowing the spin and lattice degree of freedom to be decoupled. This unique property enables e.g. anomalous Hall effect [10-11] and giant spin splitting [12] in antiferromagnetic materials. Specifically, collinear members of spin-split antiferromagnets are termed *altermagnets* due to their alternatively patterned spin polarization.

Among the many proposed altermagnets, MnTe and CrSb have emerged as key candidates due to their simple magnetic structures, high Néel temperatures, and substantial spin splitting. However, direct spectroscopic measurements of their spin textures remain scarce.

To test the predictions of altermagnetism and provide experimental insights for future applications, we performed spin-ARPES (SARPES) measurements on MnTe and CrSb at this beamtime. The results are presented in Fig. 1 and Fig. 2.

For MnTe, traces of faint bulk bands can be observed [Fig. 1(a)]. However, as shown in Fig. 1(b), SARPES measurements reveal a uniform spin-up polarization within the reliable momentum range, contradicting the theoretical expectation of an antisymmetric spin polarization around the Γ point.

For CrSb, a clear holelike band is visible [Fig. 2(a)]. S_z-resolved MDCs were subsequently measured on the bands near the Fermi level, with an energy integration window of E_B = 0 – 0.5 eV. The SARPES result shows exclusively spin-up polarization, again inconsistent with the altermagnetic theory.

To assess potential instrumental artifacts, we measured the spin polarization of polycrystalline gold, which should ideally yield zero spin signal. However, Fig. 3 reveals strong spin polarization on the gold sample, indicating a significant instrumental bias.

Given that the intrinsic spin polarization in altermagnets is inherently weak, this instrumental background likely dominates the spin signal, masking the spin polarization of the materials. This explains why Fig. 1 and Fig. 2 display similar spin polarization patterns despite their different electronic structures.

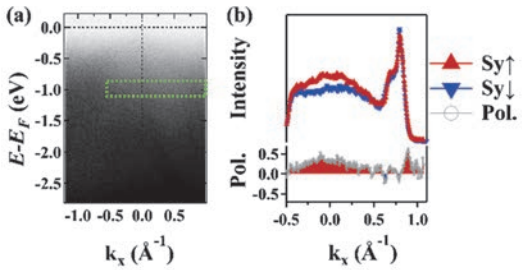

Fig. 1. The SARPES result on MnTe. (a) Spin-integrated ARPES band dispersion acquired at $h\nu$ = 74 eV (k_z = 8.5 π/c). k_x is parallel to $\bar{\Gamma}$–$\bar{M}$.Green dash frame represents the spin-MDC measurement region in (b). (b) Representative S_y-resolved MDC. Red lines with up-triangle / blue lines with down-triangle correspond to SARPES signals for opposite S_y components.

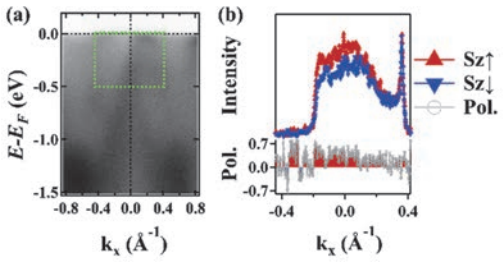

Fig. 2. The SARPES result on CrSb. (a) Spin-integrated ARPES band dispersion acquired at $h\nu$ = 45 eV (k_z = 6.5 π/c). k_x is parallel to $\bar{\Gamma}$–$\bar{M}$. Green dash frame represents the spin-MDC measurement region in (b). (b) Representative S_z-resolved MDC. Red lines with up-triangle / blue lines with down-triangle correspond to SARPES signals for opposite S_z components.

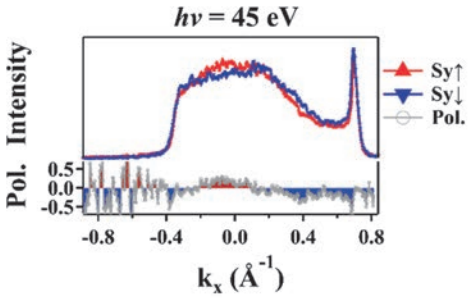

Fig. 3. Representative S_y-resolved MDC on polycrystalline Au at $h\nu$ = 45 eV, E_B = 0.5 eV.

[1] I. Žutić *et al*., Rev. Mod. Phys. **76** (2004) 323.
[2] A. Fert, Thin Solid Films **517** (2008) 2.
[3] C. Chappert *et al*., Nat. Mater. **6** (2007) 813.
[4] L.-D. Yuan *et al*., Phys. Rev. B **102** (2020) 014422.
[5] L.-D. Yuan *et al*., Phys. Rev. Mater. **5** (2021) 014409.
[6] L.-D. Yuan *et al*., Phys. Rev. B **103** (2021) 224410.
[7] S. Hayami *et al*., Phys. Rev. B **101** (2020) 220403.
[8] S. Hayami *et al*., J. Phys. Soc. Jpn. **88** (2019) 123702.
[9] C. Wu *et al*., Phys. Rev. B **75** (2007) 115103.
[10] Z. X. Feng *et al*., Nat. Electron. **5** (2022) 735.
[11] B. R. Gonzalez *et al*., Phys. Rev. Lett. **130** (2023) 036702.
[12] L. Šmejkal *et al*. Phys. Rev. X **12** (2022) 031042.

BL5U, 7U

Interfacial Heavy Fermion in Moiré Kondo Lattice $YbCu_2$/Cu(111)

T. Nakamura[1,2], H. Sugihara[2], Y. Chen[2], K. Nishihara[2], R. Ichikawa[2], H. Yamaguchi[2], K. Tanaka[3] and S. Kimura[1,2,3]

[1]*Graduate School of Frontier Biosciences, The University of Osaka, Suita 565-0871, Japan*
[2]*Department of Physics, Graduate School of Science, The University of Osaka, Toyonaka 560-0043, Japan*
[3]*Institute for Molecular Science, Okazaki 444-8585, Japan*

Heavy fermion (HF) systems originate from a translocation between localized and iterant characters due to the Kondo effect being the host of fertile exotic quantum phases of matter [1]. The Kondo lattice, where rare-earth elements containing localized *f*-electrons are periodically arranged, is the most typical system for investigating HF physics. Recently, HF in stacked layered materials with flat bands near the Fermi level (E_F), such as twisted bilayer graphene and transition metal dichalcogenides, have been actively studied [2-4]. The correlated effect at the interface leads to rich and exotic electronic quantum phases.

Among those correlated stacked systems, the moiré Kondo lattice, a coupled system of two kinds of layered materials by exchange interaction, has been proposed as a new concept in the Kondo lattice model [5-7]. The two layered materials have independent roles for the localized magnetic moment and itinerant conduction electrons. However, the interfacial HF band structure has not been observed experimentally because of poor candidates to satisfy the condition of the moiré Kondo lattice and tiny sample pieces, even in known systems. In this study, we investigated the electronic structure of a novel moiré Kondo lattice $YbCu_2$/Cu(111) by high-resolution synchrotron-based angle-resolved photoemission spectroscopy (ARPES). The $YbCu_2$/Cu(111) is the family of rare-earth-based surface alloy on noble-metal substrates with a moiré superstructure due to the lattice mismatch between the $YbCu_2$ layer with a coherence temperature of 30 K [8] and the Cu(111) substrate.

Figure 1(a) shows the high-resolution ARPES image of $YbCu_2$/Cu(111) near the Fermi level (E_F) taken with linearly polarized 33-eV photons at 15 K. Several hole bands clearly across E_F at around the $\bar{\Gamma}$ point. Note that an asymmetric photoelectron intensity of the Yb^{2+} $4f_{7/2}$ states would be due to a photoexcitation selection rule. In addition to the steep hole band at $k_x = \pm 0.05$ Å^{-1}, which is the upper branch of the 2DHF state on the $YbCu_2$ layer [8], the hole band at $k_x = \pm 0.2$ Å^{-1}, which is folded *sp*-band from Cu(111) substrate [8], was newly observed. Figure 1(b) shows the energy distribution curves of Fig. 1(a) at 0.0 Å^{-1} ($\bar{\Gamma}$ point) and 0.4 Å^{-1} where the peaks originate from the Yb^{2+} $4f_{7/2}$ states. The binding energy at the $\bar{\Gamma}$ point is slightly shifted to the higher by about 10 meV than that at 0.4 Å^{-1}. Such a momentum-dependent energy shift of the Yb^{2+} $4f_{7/2}$ state never appears in the disorder cases, such as single atom adsorption and a randomly diffused Yb atom in a Cu(111) substrate. Furthermore, the left part of the lower branch of the hole band from the Cu(111) substrate smoothly connects to the Yb^{2+} $4f_{7/2}$ flat band, pronouncing band hybridization. These results suggest that a further hybridization between the heavy fermion band of $YbCu_2$ and the bulk *sp*-band derived from Cu(111) substrate is established at the $YbCu_2$/Cu(111) interface.

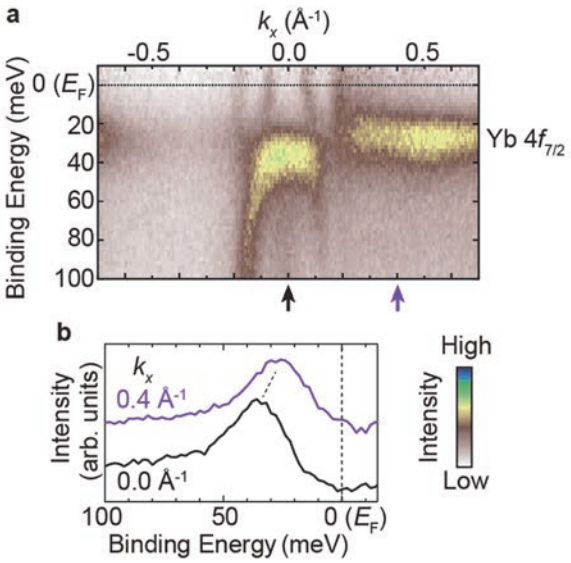

Fig. 1. (a) High-resolution ARPES image near the $\bar{\Gamma}$ point taken with linearly polarized 33-eV photons at 15 K. ARPES intensities are divided by the Fermi–Dirac distribution function convolved with the instrumental resolution. (b) Energy distribution curves at k_x = 0.0 and 0.4 Å^{-1}. The k_x positions are indicated by arrows in (a).

[1] G. R. Stewart, Rev. Mod. Phys. **56** (1984) 755.
[2] Y. Cao *et al*., Nature **556** (2018) 43.
[3] Y. Cao *et al*., Nature **556** (2018) 80.
[4] L. Wang *et al.,* Nat. Mater. **19** (2020) 861.
[5] V. Vaño *et al.,* Nature **599** (2021) 582.
[6] W. Zhao *et al.*, Nature **616** (2023) 61.
[7] W. Zhao *et al.,* Nat. Phys. **20** (2024) 1772.
[8] T. Nakamura *et al.*, Nat. Commun. **14** (2023) 7850.